Stabilizing fixed points of time-delay systems close to the Hopf bifurcation using a dynamic delayed feedback control method

2009 J. Phys. A: Math. Theor. 42 395102

(http://iopscience.iop.org/1751-8121/42/39/395102)

J. Phys. A: Math. Theor. **42** (2009) 395102 (23pp) doi:10.1088/1751-8113/42/39/395102

Stabilizing fixed points of time-delay systems close to the Hopf bifurcation using a dynamic delayed feedback control method

B Rezaie[1], **M R Jahed Motlagh**[1], **M Analoui**[1] **and S Khorsandi**[2]

[1] Iran University of Science and Technology, Narmak, Tehran, Iran
[2] Amirkabir University of Technology, Hafez St., Tehran, Iran

E-mail: brezaie@iust.ac.ir

Received 7 July 2009
Published 11 September 2009
Online at stacks.iop.org/JPhysA/42/395102

Abstract
This paper deals with the problem of Hopf bifurcation control for a class of nonlinear time-delay systems. A dynamic delayed feedback control method is utilized for stabilizing unstable fixed points near Hopf bifurcation. Using a linear stability analysis, we show that under certain conditions of the control parameters, and without changing the operating point of the system, the onset of Hopf bifurcation is delayed. Meanwhile, by applying the center manifold theorem and the normal form theory, we obtain formulas for determining the direction of the Hopf bifurcation and the stability of bifurcating periodic solutions of the closed loop system. Numerical simulations are given to justify the validity of the analytical results for the system controlled by the proposed method.

PACS numbers: 05.45.Gg, 02.30.Oz, 02.30.Ks, 02.30.Yy

1. Introduction

Time delays are an important source of performance degradation or instability in many real phenomena and a great number of engineering problems, physical systems, chemical processes and, more recently, Internet communications [1, 2]. The study of nonlinear delay differential equations (NDDEs) has received much attention over the past years. In such systems, a sequence of Hopf bifurcations may occur at the equilibrium point when a parameter of the system reaches a critical value. This may be undesirable in many systems, and control of bifurcation in order to avoid oscillations is thus an important issue. Bifurcation control generally refers to the problem of modifying the bifurcation characteristics, thereby achieving some dynamical behaviors. Some objectives of bifurcation control schemes include postponing the onset of the bifurcation, stabilizing an unstable bifurcating solution, changing the critical points of an existing bifurcation and so on [3, 4].

The delayed feedback control (DFC) method has been used to control chaos and bifurcation. DFC is well known as a method for stabilizing unstable periodic orbits (UPOs) embedded in chaotic attractors. If the delay time coincides with the period of an unstable periodic orbit, then the feedback vanishes on this orbit, see [5–9]. In addition, the DFC method is capable of stabilizing unstable fixed points (UFPs) [10–13]. The stabilization of UFPs could be more important when chaotic or periodic oscillations cause performance degradation. One of the methods of controlling UFPs, proposed by Pyragas *et al*, uses the difference between the current state and a low-pass-filtered version [10]. A DFC scheme in a diagonal coupling form has been analytically investigated using the Lambert function for the purpose of stabilizing the UFP [11, 12]. In addition, Choe *et al* have proposed two delay-coupled normal forms for Hopf bifurcations for stabilizing both UPOs and UFPs [13]. It has been shown that the DFC method is very successful in stabilizing UPOs but is less efficient in controlling UFPs in terms of stability and flexibility, especially when used for the stabilization of UFPs with large delay times due to unavoidable system dead times [14].

For many years, it was believed that the DFC method had some limitations for systems whose linearization possesses an odd number of real positive eigenvalues, and it was therefore thought that it could not be used to stabilize highly unstable systems [15–17]. In light of this, some methods were proposed to overcome this limitation. For example, it was shown that the odd number limitation of the DFC method could be overcome by including an additional unstable mode in the feedback loop [18]. Recently, it has been demonstrated that this so-called odd number limitation does not hold true for autonomous systems controlled by DFC [19, 20]. However, it does still hold true for stabilizing UFPs [21]. Moreover, if the Jacobian matrix at a UFP has a characteristic exponent with a zero real part, the UFP cannot be stabilized by linear DFC with arbitrary delayed time [22]. As a result, DFC can be used to stabilize only a class of unstable systems [17]. In addition, there is a finite range of values of feedback gain at which the control can be achieved [23].

The DFC method has also been used to control time-delay systems [9, 24–28]. We propose a dynamic delayed feedback control (DDFC) method based on a washout filter [16] in order to control UFPs at the Hopf bifurcation point. A washout filter is a high-pass filter that rejects steady-state inputs, while passing transient inputs. The method allows for a noninvasive stabilization of UFPs for time-delay systems, i.e. it has the advantage of not changing the location of the equilibrium point of the open-loop system and thereby, stabilization is achieved by a small control energy. The so-called odd number limitation of the DFC method for the case of UFP stabilization can be overcome by using the proposed method, and therefore the stabilization of a much larger class of systems will be possible. We also obtain deeper analytical insight into the DDFC by discussing the stability domain in the space of the control parameters. In comparison with DFC, the efficiency of the control can be improved, since the regions in the parameter space in which the fixed point is stabilized can be extended and the range of values of the feedback gain can be increased.

The center manifold theorem and normal form theory are useful tools for investigating nonlinear dynamical systems and are often applied to control systems in order to consider instability and bifurcation control [3, 29, 30]. Based on the closed form of the Hopf bifurcation calculation in [31], we also derive formulas for determining the direction of the Hopf bifurcation and the stability of the bifurcating periodic solutions of the closed loop system.

As an application, we concentrate on an Internet congestion control system that is modeled by NDDEs [32–34]. The basic aim of the Internet congestion control system is to adjust the sending rates of source hosts in order to avoid congestion at links. It has been shown that this system exhibits Hopf bifurcation when a system parameter varies [35–40]. This leads to undesirable oscillations in the transmission rates of sources, which causes underutilization of links and thereby, a significant degradation in network performance. There are some works dealing with delayed feedback control of Hopf bifurcations [41–43] in this system. The aim of bifurcation control schemes in the congestion control system is to absorb oscillations in order to provide an improvement in network performance. We study the control of Hopf bifurcation using the DDFC method for a rate-based Kelly's model of an Internet congestion control system [32]. Simulation results for a typical scenario demonstrate the applicability of the method.

The paper is organized as follows. In section 2, we consider a Hopf bifurcation analysis for the closed loop system. The properties of Hopf bifurcation is studied in section 3. In order to verify the analytical results, the simulation results are presented in section 4. Finally, conclusions are drawn in section 5.

2. Hopf bifurcation analysis

2.1. The model

In this paper, we consider a class of time-delay systems described by a first-order equation of the form

$$\dot{x}(t) = f\left(x(t-\tau)\right), \tag{1}$$

where $x(t) \in \Re$ is the state variable, τ is a positive delay parameter and $f(\cdot)$ is a nonlinear continuously differentiable function. We assume that there exists an equilibrium point $x^* \neq 0$ such that $b = f'(x^*) < 0$.

By simple calculations, one can find that for $\tau_c = -\pi/2f'(x^*)$, a Hopf bifurcation occurs at the equilibrium x^* of the system (1). Our goal is to change this critical value in order to delay the Hopf bifurcation occurrence, and thereby drive the system toward desirable behavior. A famous approach that achieves the same goal is DFC with the following control structure:

$$\dot{x}(t) = f\left(x(t-\tau)\right) + a[x(t) - x(t-\tau)]. \tag{2}$$

For $a>b/2$, it undergoes a Hopf bifurcation at $\tau_{c1} = \frac{1}{\omega_0}\cos^{-1}\left(\frac{a}{a-b}\right)$, where $\omega_0 = \sqrt{(b-a)^2 - a^2}$. Since $\tau_{c1} > \tau_c$, the DFC can delay the Hopf bifurcation for $a \in (b/2, 0)$.

In this paper, we improve some dynamical properties of the DFC method, such as the domain of stability in parameter space. We propose a dynamic compensation for a general model of time-delay systems in order to control Hopf bifurcation with a minimum control effort. In order to improve the DFC method, we add a dynamic feedback to the system controlled by DFC. Thus, we have the following control system:

$$\begin{aligned} \dot{x}(t) &= f(x(t-\tau)) + a[x(t) - x(t-\tau)] + u(t) \\ \dot{u}(t) &= a[x(t) - x(t-\tau)] - \mathrm{d}u(t), \end{aligned} \tag{3}$$

where *u*(*t*) is the control law, *a* and *d* are the control parameters and the function $f(\cdot)$ satisfies the same conditions assumed for (1). We also assume that *d* is a positive parameter.

Using Taylor expansion and letting $y_1(t) = x(t) - x^*$ and $y_2(t) = u(t)$, we can expand the right-hand side of equation (3) around x^*, resulting in the following equation:

$$\begin{aligned} \dot{y}_1(t) &= ay_1(t) + (b-a)y_1(t-\tau) + y_2(t) + \tfrac{1}{2}b_2y_1^2(t-\tau) + \tfrac{1}{6}b_3y_1^3(t-\tau) + O\left(y_1^4(t-\tau)\right) \\ \dot{y}_2(t) &= ay_1(t) - ay_1(t-\tau) - \mathrm{d}y_2(t), \end{aligned} \tag{4}$$

where $b = f'(x^*) < 0$, $b_2 = f''(x^*)$ and $b_3 = f'''(x^*)$. The characteristic equation is

$$Q(\lambda,\tau) := \det\begin{pmatrix}\lambda - b\,\mathrm{e}^{-\lambda\tau} - a(1-\mathrm{e}^{-\lambda\tau}) & -1\\ -a(1-\mathrm{e}^{-\lambda\tau}) & \lambda + d\end{pmatrix}$$
$$= \lambda^2 + [(d-a) - (b-a)\,\mathrm{e}^{-\lambda\tau}]\lambda - a(d+1) + [a(d+1) - bd]\,\mathrm{e}^{-\lambda\tau}. \qquad (5)$$

Considering τ as the bifurcation parameter and using the distribution of the roots of the characteristic equation (5), we determine some restrictions on the system and control parameters under which the Hopf bifurcation occurs. We study the application of the Hopf bifurcation theorem for the closed loop system (3) by the following theorem.

Theorem 1. *If the control parameters a and d satisfy* $bd[2a(d+1) - bd] < 0$*, then we have the following.*

(i) Equation (5) exhibits a Hopf bifurcation for $\tau = \tau_0$*, where*

$$\tau_j = \frac{1}{\omega_0}\cos^{-1}\left[\frac{a(a-b+1)\omega_0^2 + a(d+1)[a(d+1)-bd]}{(b-a)^2\omega_0^2 + [a(d+1)-bd]^2}\right] + \frac{2j\pi}{\omega_0}, \qquad \textit{for} \quad j = 0, 1, \ldots$$

and $\omega_0 = \frac{\sqrt{2}}{2}(A + \sqrt{A^2 - 4B})^{1/2}$ *for* $A = b^2 - d^2 - 2a(b+1)$ *and* $B = bd[2a(d+1) - bd]$.

(ii) For $\tau < \tau_0$*, all roots of (5) have strictly negative real parts.*

Proof. The proof is provided in appendix A. □

Therefore, the closed loop system undergoes Hopf bifurcation when the delay parameter passes through a critical value τ_0. It is not difficult to show that $\tau_0 > \tau_c$, i.e. that the controller postpones the Hopf bifurcation occurrence.

We now investigate the range of the control parameters for which Hopf bifurcation may occur. Consider a two-dimensional space of parameters in the (a, d)-plane in order to show the domain of stability of the fixed point for the closed loop system. In figure 1, inside the gray region, the fixed point is stable and no oscillations occur. In the unstable area, there is a critical value τ_0 for which the Hopf bifurcation occurs. The boundary of the stable region satisfies $2a(d+1) - bd = 0$. In addition, the area to the left of the dashed line at $a = b/2$ represents the stability domain for the system controlled by the DFC method. Therefore, the stable area has increased using the proposed DDFC method.

Now, consider the following corollary.

Corollary 1. *If* $a(d+1) = bd$, $a < 0$ *and* $d > -b > 0$*, then the closed loop system (3) is locally asymptotically stable.*

Proof. Consider characteristic equation (5). For $\tau = 0$, the closed loop system is locally asymptotically stable (see appendix A). For $\tau \neq 0$, assuming $\lambda = \pm\mathrm{i}\,\omega$ with $\omega > 0$, we obtain

$$Q(\mathrm{i}\,\omega,\tau) = [-\omega^2 - (b-a)\omega\sin\omega\tau - bd] + \mathrm{i}\,\omega[(d-a) - (b-a)\cos\omega\tau].$$

Since $a < 0$, $d > -b > 0$ and $a(d+1) = bd$, thus

$$\mathrm{im}\{Q(\mathrm{i}\,\omega,\tau)\} = \omega[(d-a) - (b-a)\cos(\omega\tau)] \geqslant \omega(d+b) > 0,$$

and therefore we have $Q(\mathrm{i}\,\omega,\tau) \neq 0$. According to lemma (A.1), this proves that the system (3) is locally asymptotically stable. □

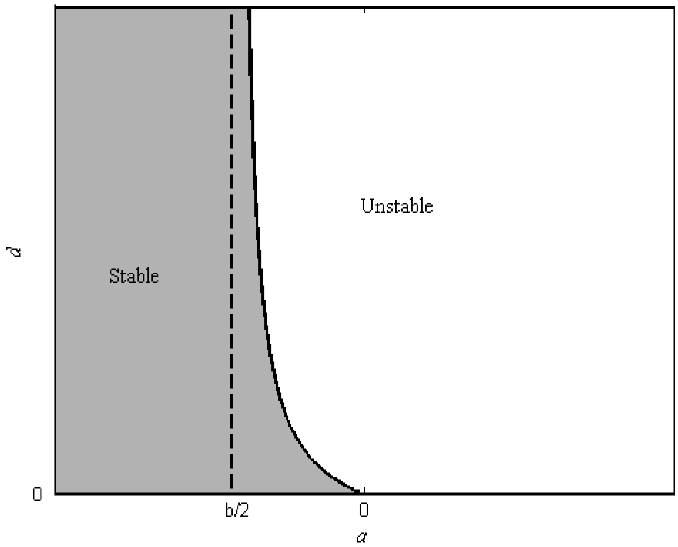

Figure 1. The stability domain of the closed loop system in the (a, d)-plane.

Corollary 1 gives the condition on the controller parameters under which the Hopf bifurcation is avoided for all values of the delay parameter.

Remark 1. To utilize the proposed method in this paper for stabilizing UPOs, we can use the following controller:

$$\begin{aligned} \dot{x}(t) &= f(x(t-\tau)) + a[x(t) - x(t-T)] + u(t) \\ \dot{u}(t) &= a[x(t) - x(t-T)] - \mathrm{d}u(t). \end{aligned} \tag{6}$$

We use the fact that the period of the periodic orbits (stable or unstable) originating at the bifurcation critical value $\tau = \tau_0$ is $2\pi/\omega_0$. Thus, we must set $T = 2\pi/\omega_0$. Furthermore, we set $d = -b\,\mathrm{e}^{-\omega_0\tau_0}$. Consequently, $\lambda = \mathrm{i}\,\omega_0$ is a root of (5) as well as the characteristic equation of the open loop system. Thus, we propose to choose such a T as to stabilize the UPO. Hence, for such a T, $\tau = \tau_0$ is a Hopf bifurcation critical value for (6), and the stability of the periodic solution arising from this Hopf bifurcation is dependent on a. Accordingly, by a suitable choice of a, the UPO may become stable. It is easy to verify that if $\lambda(\tau, T, d) = \alpha(\tau, T, d) + \mathrm{i}\,\omega(\tau, T, d)$ denotes a root of (5) near $\tau = \tau_0$, $T = 2\pi/\omega_0$ and $d = -b\,\mathrm{e}^{-\omega_0\tau_0}$, then

$$\frac{\partial\alpha(\tau_0, 2\pi/\omega_0, -b\,\mathrm{e}^{-\omega_0\tau_0})}{\partial\tau} \neq 0, \qquad \frac{\partial\alpha(\tau_0, 2\pi/\omega_0, -b\,\mathrm{e}^{-\omega_0\tau_0})}{\partial T} \neq 0,$$

$$\frac{\partial\alpha(\tau_0, 2\pi/\omega_0, -b\,\mathrm{e}^{-\omega_0\tau_0})}{\partial d} \neq 0.$$

Therefore, the system (6) undergoes Hopf bifurcation at the equilibrium point x^*, when $\tau = \tau_0$, $T = 2\pi/\omega_0$ and $d = -b\,\mathrm{e}^{-\omega_0\tau_0}$. Note that we must choose a such that for $\tau = \tau_0$, $T = 2\pi/\omega_0$ and $d = -b\,\mathrm{e}^{-\omega_0\tau_0}$, all roots of (5) except for $\pm\mathrm{i}\,\omega_0$ have negative real parts, and the corresponding periodic solution becomes stable.

2.2. Application

The interest in studying the system (1) is justified by the fact that it includes many models that have been intensively and extensively studied in the literature. In order to illustrate the effectiveness of the proposed control method, we concentrate on an application of the model (1) in a simplified fluid approximation of an Internet congestion control proposed by Kelly [33]. The model is described by the following equation:

$$\dot{x}(t) = \kappa[w - x(t-\tau)p(x(t-\tau))], \tag{7}$$

where $x \in \Re$ is the state variable, $\kappa, w, \tau > 0$ are the system parameters and $p(\cdot)$ is a positive and strictly increasing function. It has been shown that such delayed systems exhibit Hopf bifurcation when the nonlinear function satisfies a particular set of conditions [35, 37, 41, 42]. Note that the positive equilibrium of the system (7) is x^*, which satisfies $x^*p(x^*) = w$. The parameter b for this system is defined by

$$b = f'(x^*) = -\kappa[p(x^*) + x^*p'(x^*)] < 0.$$

Equation (7) has been used for a data network that consists of a source with a transmission rate $x(t)$ and that utilizes a single link. The link as the resource of the network charges a price per unit $p(x)$, where $p(\cdot)$ is a function of the rate going through the link. The price of the resource may depend on link congestion, loss probability, etc. Due to link propagation, there is a reverse delay τ of the feedback signal from the resource to the user. In addition, κ is the gain parameter, and w is the willingness to pay. Each user/source adjusts its rate based on the feedback provided by the resource/link in the network to equalize its willingness to pay and the price of the link.

We now illustrate how the control parameters of the DDFC method influence the critical value of delay for the system (7). The bifurcation point τ_0 in the DFC method depends on the control parameter a. In the DDFC method, it depends on the control parameters a and d. Figure 2 shows the stability boundaries by comparing the curves $\tau_0(a)$ as parameter a is varied. One can observe that for each fixed value of d, by decreasing the control parameter a toward $-\infty$, the critical value of delay has been increased using the proposed method and therefore the Hopf bifurcation has been postponed. This means that those points which were unstable in the system controlled by the DFC method are now stable as they are moved by the control action to the area below the new stability boundary. Furthermore, it is possible to raise the stability boundary by decreasing the parameter d for each fixed value of a.

To provide insight into how the proposed control method works, let us consider the problem of stabilizing the fixed point of (3). The characteristic equation reads

$$1 - aG(\lambda) = 0,$$

where $G(\lambda) = \frac{(\lambda+d+1)(1-e^{-\lambda\tau})}{(\lambda+d)(\lambda-b\,e^{-\lambda\tau})}$. For the DFC method, we have $G(\lambda) = \frac{1-e^{-\lambda\tau}}{\lambda-b\,e^{-\lambda\tau}}$. Therefore, we have added a pair of stable pole and zero to the DFC method, which increases the stability region of the closed loop system. To compare these methods, we illustrate the effect of the parameter a on the stability of the system in two methods. For DFC method, this can be seen in the root loci in figure 3(*a*) as the parameter a varies from 0 to $-\infty$. For $a = 0$, there are two eigenvalues with positive real part. This means that the controlled system is unstable. With the decrease of a toward $-\infty$, the largest eigenvalue approaches the imaginary axis at $a = -0.64$. For $a < -0.64$, the closed loop system is stable. The corresponding stability domain is shown in figure 3(*b*).

For the proposed method, the corresponding results are shown in figure 4. It is clearly seen that for $a < -0.46$, the closed loop system is stable. Therefore, the region of the control parameter a ensuring the stability of the closed loop system has increased.

In addition, the largest real parts of the complex eigenvalues λ as a function of the delay parameter τ are shown in figures 5 and 6. Comparing the domains of control in figures 5 and 6(*a*), it can be seen that for each fixed value of a, the fixed point of the proposed DDFC method can stabilize the system in a larger range of τ. In addition, figure 6(*b*) shows that

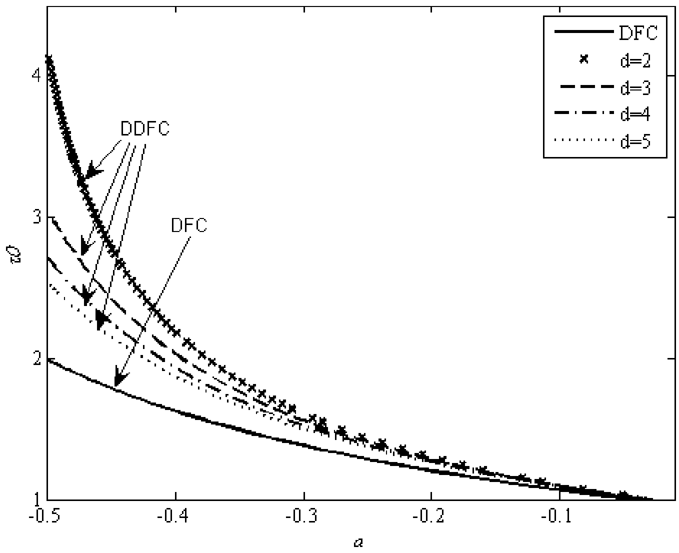

Figure 2. The curves τ_0 (a) for the closed loop system with $b = -1.63$.

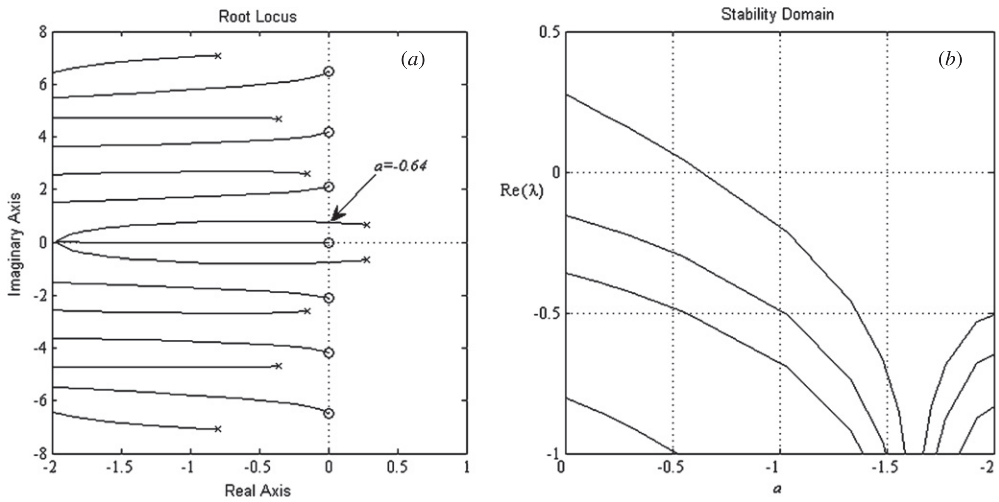

Figure 3. (*a*) Root loci of the closed loop system controlled by the DFC method. (*b*) Re(λ) versus *a* for $b = -1.63$ and $\tau = 3$.

by decreasing the control parameter *d*, the real part of the leading eigenvalue becomes more negative.

3. Direction and stability of Hopf bifurcation

The direction of the Hopf bifurcation and the stability and period of the periodic solution bifurcating from the equilibrium, as stated in [31], are interesting issues. In this section, based on the normal form method and the center manifold theorem introduced by Hassard *et al* [31],

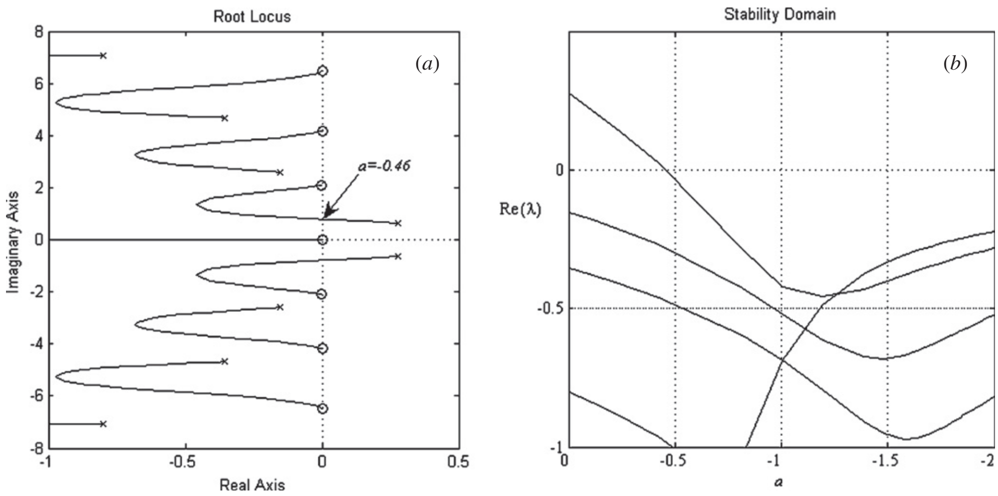

Figure 4. (*a*) Root loci of the closed loop system for the DDFC method. (*b*) Re(λ) versus *a*. Parameters: $b = -1.63$, $d = 2$ and $\tau = 3$.

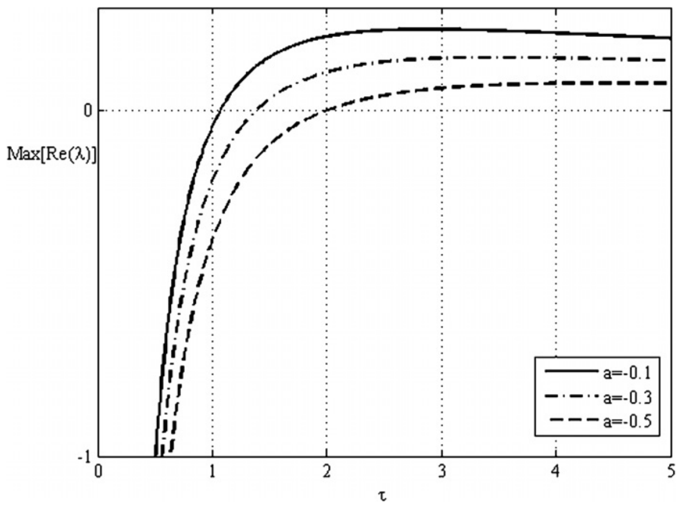

Figure 5. The largest Re(λ) versus τ for the DFC method with $b = -1.63$.

we will determine the Hopf bifurcation properties of the system (3) at the critical value τ_0. According to the center manifold theorem, near the equilibrium point, there is a family of smooth invariant manifolds preserving the inherited dynamics of the original systems. Hence, we can use the normal form to analytically describe the bifurcation.

To determine the Hopf bifurcation, it is important to obtain the normal form first, and then determine the signs of its parameters. The normal form can be found using the center manifold reduction as the key component of the Hopf bifurcation calculations (see appendix B for details). The dynamics of the system (3) is topologically equivalent to the following equation at the sufficiently small neighborhood of the Hopf bifurcation point:

$$\dot{z} = \mathrm{i}\,\omega_0 z + g(z, \bar{z}) = \mathrm{i}\,\omega_0 z + g_{20}\frac{z^2}{2} + g_{11} z\bar{z} + g_{02}\frac{\bar{z}^2}{2} + g_{21}\frac{z^2\bar{z}}{2} + \cdots, \tag{8}$$

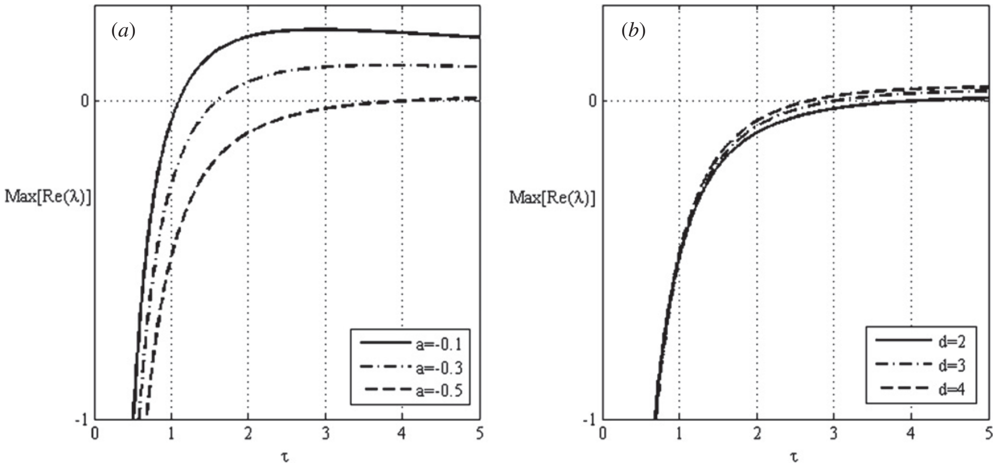

Figure 6. The largest Re(λ) versus τ for the DDFC method with $b = -1.63$, (*a*) for different values of a with $d = 2$, (*b*) for different values of d with $a = -0.5$.

where z and $\bar{z}$ are the local coordinates for the center manifold. The values of g_{20}, g_{11}, g_{02} and g_{21} are computed according to the formulas derived in appendix B. Thus, we can calculate all of the following quantities which are required for the stability analysis of Hopf bifurcation:

$$
\begin{aligned}
C_1(0) &= \frac{\mathrm{i}}{2\omega_0}\left(g_{20}g_{11} - 2\,|g_{11}|^2 - \frac{1}{3}\,|g_{02}|^2\right) + \frac{g_{21}}{2} \\
\mu_2 &= -\frac{\mathrm{Re}\{c_1(0)\}}{\mathrm{Re}\lambda'(0)} \\
\tau_2 &= -\frac{\mathrm{Im}\{C_1(0)\} + \mu_2 \mathrm{Im}\lambda'(0)}{\omega_0} \\
\beta_2 &= 2\,\mathrm{Re}\{C_1(0)\}.
\end{aligned}
\tag{9}
$$

The periodic solutions and their stabilities can be analyzed with the aid of the normal form parameters $C_1(0)$, μ_2, β_2 and τ_2. Using the result of [31], we state the conditions for the stability analysis of Hopf bifurcation by the following theorem.

Theorem 2. *Let $C_1(0)$, μ_2, β_2 and τ_2 be given in (9) as calculated in appendix B. Then,*

(i) the bifurcation solutions exist for $\tau = \tau_0$: if $\mu_2 > 0$, then the bifurcation is supercritical, and if $\mu_2 < 0$, then the bifurcation is subcritical;
(ii) β_2 determines the stability of the bifurcating periodic solutions: the solutions are orbitally stable if $\beta_2 < 0$ and unstable if $\beta_2 > 0$; and
(iii) τ_2 determines the period of the bifurcating periodic solutions: the period increases if $\tau_2 > 0$ and decreases if $\tau_2 < 0$.

Note that the period of the bifurcation solution can be determined by

$$\tilde{T}(h) = \frac{2\pi}{\omega_0}(1 + h^2\tau_2 + \cdots).$$

For $\tau = \tau_0$ (or equivalently, $h = 0$), the period of the closed loop system will be $\tilde{T} = 2\pi/\omega_0$. In addition, by determining the normal form, we are able to calculate the amplitude of the bifurcating orbits at $\tau = \tau_0$.

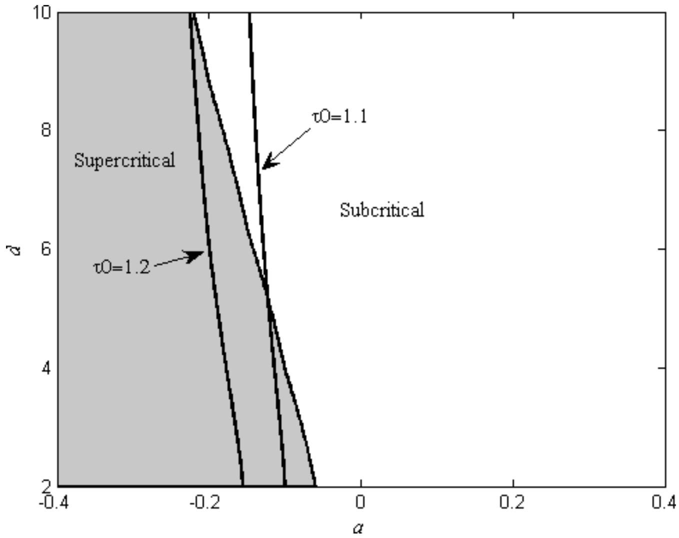

Figure 7. Domain of Hopf bifurcation stability in the (a, d)-plane. The shaded area indicates combinations of a and d, for which the Hopf bifurcation is supercritical ($\mu_2 > 0$). The curves show the ranges of control parameters while the delay is fixed at critical values $\tau_0 = 1.1$ and $\tau_0 = 1.2$.

We now investigate the effects of the control parameters on the normal form parameters for the model (7) controlled by the proposed method. Suppose that the conditions of the Hopf bifurcation occurrence hold and the model has a periodic solution. We also assume that $b = -1.6361$, $b_2 = -0.1264$ and $b_3 = 0.1069$. Figure 7 shows the stability domain of the periodic orbit in the plane of control parameters (a, d). In addition, the curves $d(a)$ are shown in figure 7 for two different values of τ_0. One can see that using the proposed control method the stability of periodic solution is affected in such a way that the Hopf bifurcation can be changed from subcritical to supercritical as the control parameters change.

Therefore, an appropriate choice of the control parameters can stabilize the periodic orbit without changing the operating point and the critical value of delay. This suggests that the proposed method can perform as an efficient method for stabilization of the solution at Hopf bifurcation, and a transition from subcritical Hopf bifurcation to supercritical Hopf bifurcation will be possible.

4. Simulations

In this section, numerical results are presented for an example used in [37], which is a proportionally fair congestion control system (7) for a simple network including a single source that uses a single link. Let the target parameter be $\omega = 1$ and the gain parameter be $\kappa = 3/2$. In addition, consider the link to utilize a random early marking (REM) mechanism [44] as a price function with the same parameters in [37]. The REM mechanism marks a packet with drop probability $p(x) = 1 - \mathrm{e}^{-x}$ per unit of flow rate. Therefore, the congestion control system takes the following form:

$$\dot{x}(t) = \tfrac{3}{2}\left[1 - x(t-\tau) + x(t-\tau)\,\mathrm{e}^{x(t-\tau)}\right]. \tag{10}$$

First, consider the open loop system (10) and let the delay parameter be the bifurcation parameter. The equilibrium point of (10) is $x^* = 1.35$. Figure 8 shows the simulation results

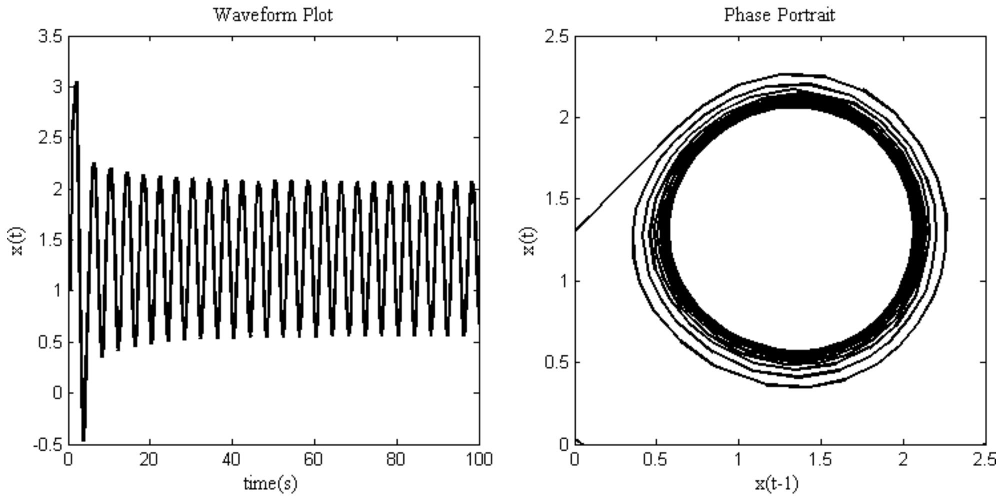

Figure 8. Waveform plot and phase portrait of an uncontrolled system with $\tau = 1$.

for the open loop system with $\tau = 1$. We can see that the system is not stable and that there exists a Hopf bifurcation. In addition, as in [37], we have

$$\tau_c = 0.9601, \qquad \omega_0 = 1.6361$$

and

$$D_2 = 0.0526, \qquad \omega_2 = -0.909, \qquad \eta_2 = -0.0318.$$

The parameters D_2, ω_2 and η_2 are defined in [37]. The system loses its stability when the delay passes through the critical value τ_c, and Hopf bifurcation occurs. Since $D_2 > 0$, the bifurcation is supercritical, and because $\eta_2 < 0$, the periodic orbits are locally asymptotically stable. Furthermore, since $\omega_2 > 0$, the periodic solutions increase as τ increases.

Now, we apply the proposed DDFC method to the system (10) in order to delay the Hopf bifurcation. We consider the closed loop system (3) with initial condition $x_0 = 1$ and control parameters $a = -0.5$ and $d = 5$. Therefore, we have

$$\tau_0 = 2.3054, \qquad \omega_0 = 0.8673$$

and

$$\mu_2 = 0.6839, \qquad \tau_2 = 0.3490, \qquad \beta_2 = -0.1345.$$

Thus, the critical value for Hopf bifurcation increases from 0.9601 to 2.3054, implying that the onset of the Hopf bifurcation is postponed. In addition, since $\mu_2 > 0$, the bifurcation is supercritical and, because $\tau_2 > 0$, the periodic solutions increase as τ increases. Furthermore, the periodic orbit is stable since $\beta_2 < 0$. Figures 9 and 10 show the simulation results for $\tau = 1.5$ and $\tau = 2.5$. We can observe that the system is locally asymptotically stable when $\tau < \tau_0$ and that is not stable when $\tau > \tau_0$. It is obvious that for $\tau < \tau_0$ the controlled system converges to the same equilibrium point as the original system. Furthermore, there is no control signal when the rate signal converges to its final value.

The parameters a and d can be used to tune the onset of the Hopf bifurcation or the Hopf bifurcation properties defined by parameters μ_2, τ_2 and β_2. Using different values of a and d, one can efficiently delay the onset of the Hopf bifurcation or change the stability, direction and

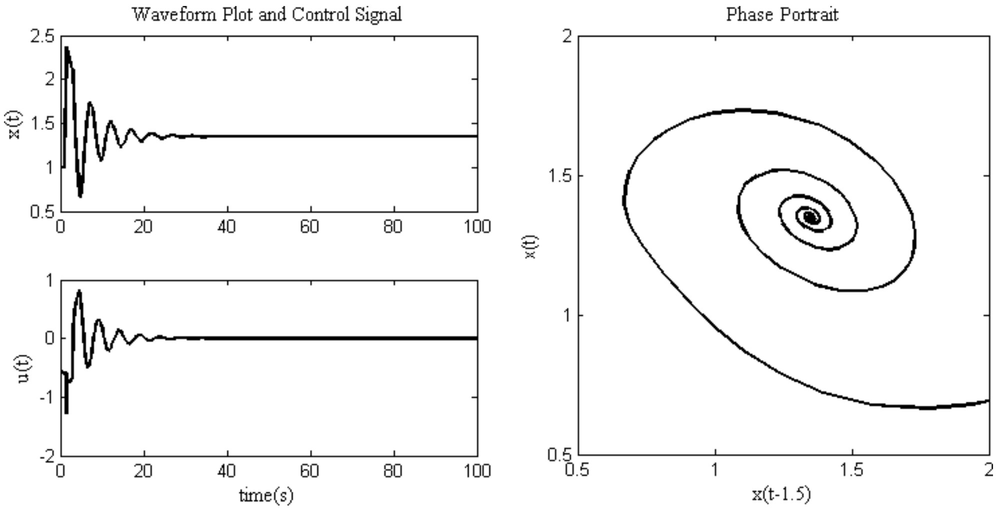

Figure 9. Waveform plot, control signal and phase portrait of a closed loop system with $\tau = 1.5$, $a = -0.5$ and $d = 5$.

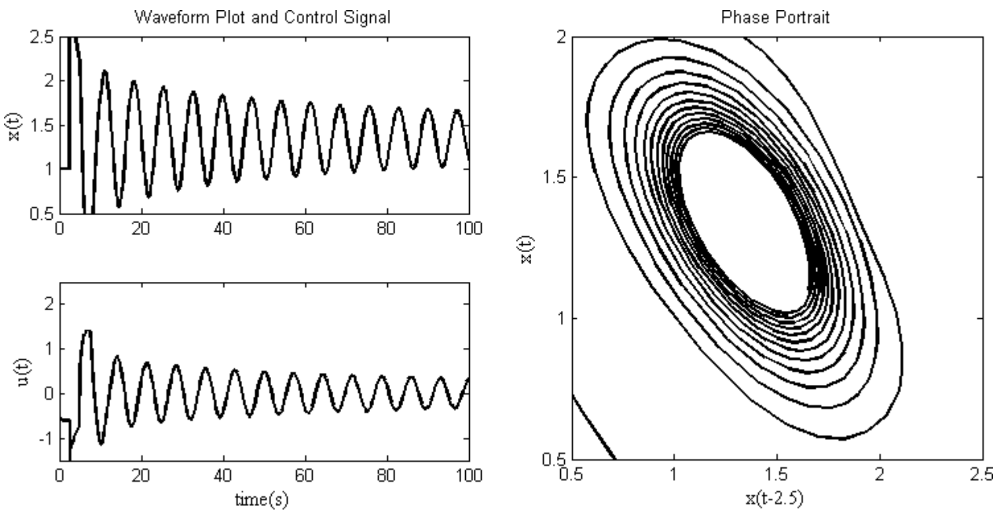

Figure 10. Waveform plot, control signal and phase portrait of a closed loop system with $\tau = 2.5$, $a = -0.5$ and $d = 5$.

period of the Hopf bifurcation. In addition, by appropriately selecting the control parameters, the bifurcation can be avoided for all values of the delay parameter. Let the control parameters be $a = -1.09$ and $d = 2$. Figures 11 and 12 show the stability of the system for $\tau = 2.5$ and $\tau = 10$, and testify the theoretical results in corollary 1. It can be shown that with this controller, the system is locally asymptotically stable for all values of τ which implies that the controlled system is robust against delay variations.

We now study the behavior of the closed loop system for a different initial condition but close to the fixed point. Figure 13 shows that the control mechanism is successful for initial condition $x_0 = 4$. However, the success of the control depends sensitively on the initial

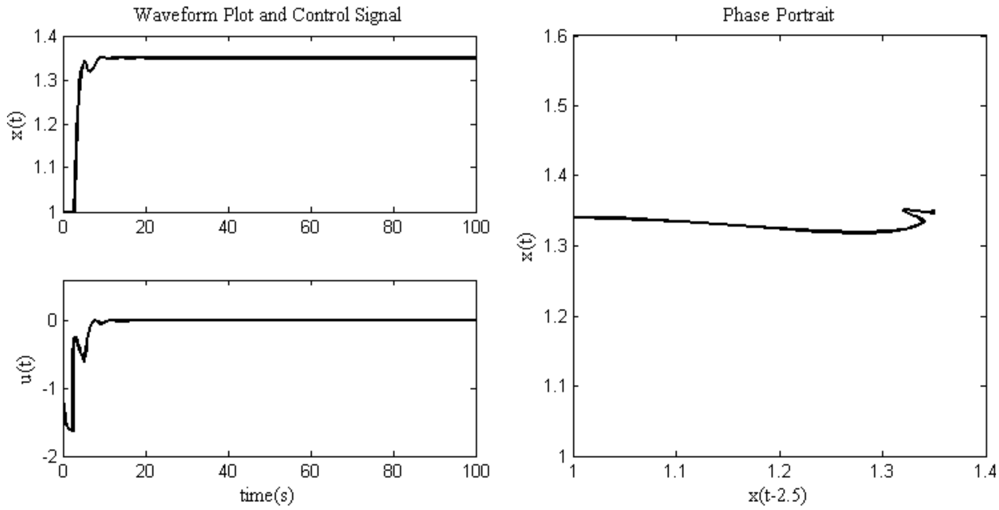

Figure 11. Waveform plot, control signal and phase portrait of a closed loop system with $\tau = 2.5$, $a = -1.09$ and $d = 2$.

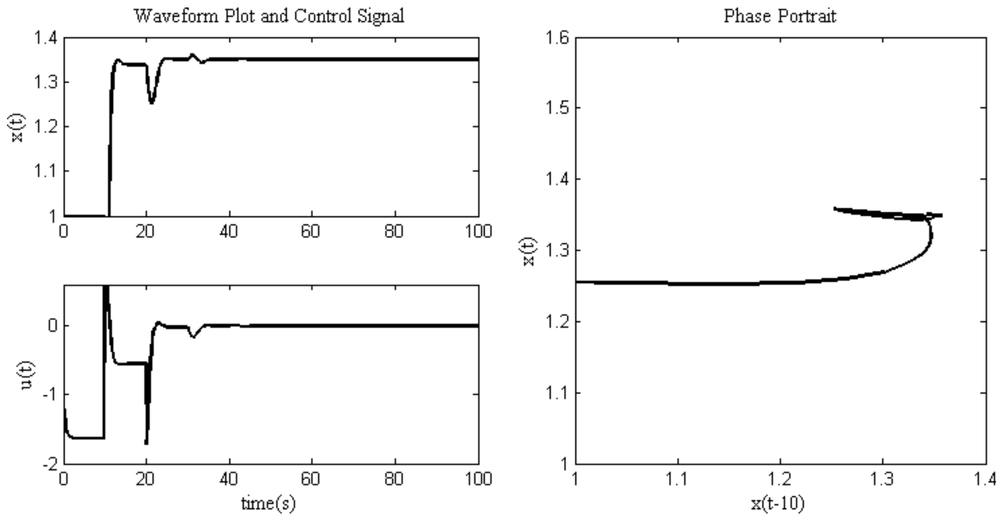

Figure 12. Waveform plot, control signal and phase portrait of a closed loop system with $\tau = 10$, $a = -1.09$ and $d = 2$.

condition. When applying a linear method, control is obtained only for a small range of initial conditions close to the fixed point. Starting from initial conditions outside this small range, the controller variable may escape to infinity.

Finally, to investigate the robustness of the method against noise, we simulate the results in the presence of white noise in the measure signal $x(t)$. Figure 14 shows that white noise and inaccuracy in the measurements affect the system response. This observation, in fact, shows that the method may lose its accuracy in the presence of noise. However, the value of the signal rate is still bounded.

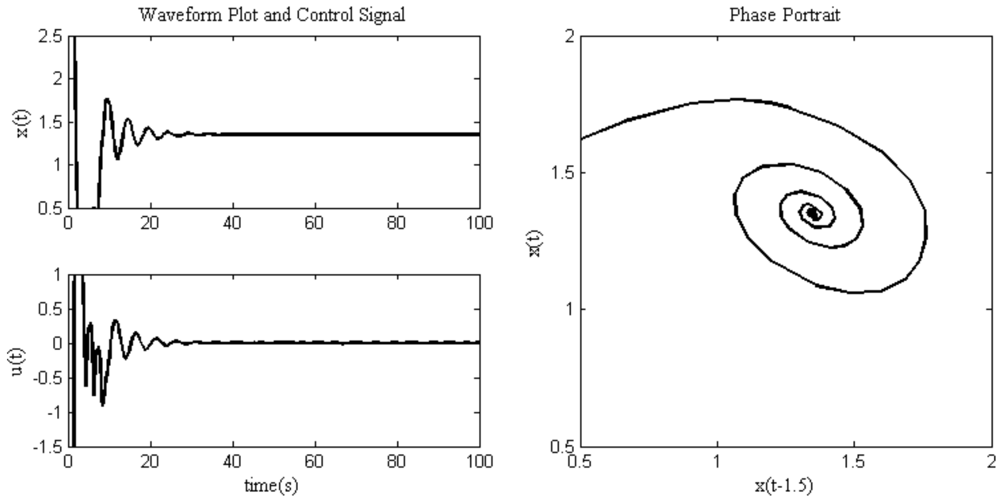

Figure 13. Waveform plot, control signal and phase portrait of closed loop system with $\tau = 1.5$, $a = -0.5$ and $d = 5$ with the initial condition $x_0 = 4$.

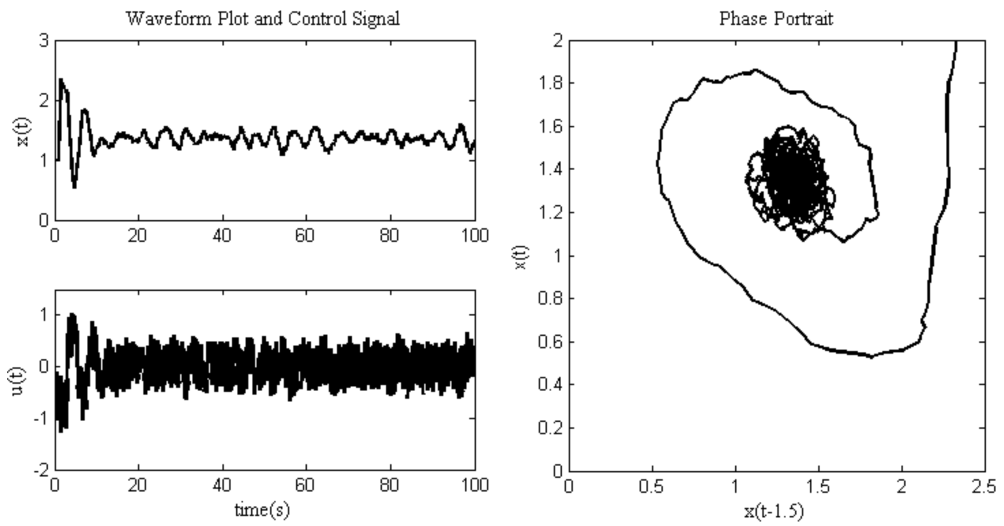

Figure 14. Waveform plot, control signal and phase portrait of a closed loop system with $\tau = 1.5$, $a = -0.5$ and $d = 5$ in the presence of white noise in the measure signal $x(t)$.

5. Conclusion

The Hopf bifurcation control problem was considered for a class of nonlinear time-delay systems. A dynamic delayed feedback control method was proposed in order to retard the Hopf bifurcation occurrence. The proposed method preserved the operating point of the system, i.e. the control action vanished once stability was achieved. By choosing the delay parameter as a bifurcation parameter and using linear stability analysis, we determined the condition for Hopf bifurcation occurrence for the controlled system. We also applied a method based on the center manifold theorem and normal form theory to study the Hopf bifurcation properties. By selecting appropriate control parameters, the proposed controller can effectively postpone the onset of the Hopf bifurcation or change the properties of the Hopf bifurcation. An application of the proposed control system in a model of an Internet congestion control system was studied. Numerical simulations for a congestion control system in a simple network were presented to justify the analytical results. The proposed control method may be extended in order to study higher dimensional nonlinear time-delay systems.

Acknowledgments

The authors thank the anonymous reviewers for their constructive comments that helped to improve the paper. This work was supported in part by the Iran Telecommunication Research Center (ITRC).

Appendix A. Proof of theorem 1

Hopf bifurcation occurrence requires that the characteristic equation (5) has a simple pair of purely imaginary roots, and the eigenvalues cross the imaginary axis with a non-zero velocity (transversality condition), i.e. $\mathrm{Re}\left(\frac{\mathrm{d}\lambda(\tau_0)}{\mathrm{d}\tau}\right) \neq 0$, where $\tau_0 > 0$ is the critical value of τ.

We derive the condition for Hopf bifurcation occurrence by setting the real part of the roots of the characteristic equation (5) equal to zero, i.e. $\lambda = \pm \mathrm{i}\,\omega_0$, where $\omega_0 > 0$. Substituting this into (5), and separating real and imaginary parts of the resulting equation, we obtain the solution of equation (5) as follows:

$$\begin{aligned} &-(b-a)\omega_0 \sin(\omega_0\tau) + [a(d+1) - bd]\cos(\omega_0\tau) = a(d+1) + \omega_0^2 \\ &(b-a)\omega_0 \cos(\omega_0\tau) + [a(d+1) - bd]\sin(\omega_0\tau) = (d-a)\omega_0 \end{aligned} \tag{A.1}$$

which leads to

$$\omega_0^4 + [2a(b+1) + d^2 - b^2]\omega_0^2 + bd[2a(d+1) - bd] = 0. \tag{A.2}$$

It is easy to see that if the condition $bd[2a(d+1) - bd] < 0$ holds, then equation (A.2) has only one positive root as follows:

$$\omega_0 = \sqrt{\frac{-[2a(b+1)+d^2-b^2] + \sqrt{[2a(b+1)+d^2-b^2]^2 - 4bd[2a(d+1)-bd]}}{2}}.$$

Thus, one can determine

$$\tau_j = \frac{1}{\omega_0}\cos^{-1}\left[\frac{a(a-b+1)\omega_0^2 + a(d+1)[a(d+1)-bd]}{(b-a)^2\omega_0^2 + [a(d+1)-bd]^2}\right] + \frac{2j\pi}{\omega_0}, \quad \text{for} \quad j = 0, 1, \ldots, \tag{A.3}$$

where the non-negative integer j takes care of the different leaves of the involved multivalued function [46–48]. Therefore, the characteristic equation (5) with $\tau = \tau_j$ $\{j = 0, 1, 2, \ldots\}$ has a pair of imaginary roots $\lambda = \pm \mathrm{i}\omega_0$, which are simple.

Now, applying the implicit function theorem, we obtain

$$\left[\frac{\mathrm{d}\lambda(\tau)}{\mathrm{d}\tau}\right]^{-1} = \frac{[2\lambda + (d-a)]\,\mathrm{e}^{\lambda\tau}}{\lambda[(a-b)\lambda + a(d+1) - bd]} + \frac{(a-b)}{\lambda[(a-b)\lambda + a(d+1) - bd]} - \frac{\tau}{\lambda}. \tag{A.4}$$

Since $\lambda(\tau_0) = \mathrm{i}\,\omega_0$, we have

$$\mathrm{Re}\left\{\left[\frac{\mathrm{d}\lambda(\tau_0)}{\mathrm{d}\tau}\right]^{-1}\right\} = \mathrm{Re}\left\{\frac{[(d-a)\cos(\omega_0\tau_0) - 2\omega_0\sin(\omega_0\tau_0)]}{(b-a)\omega_0^2 + \mathrm{i}\,\omega_0[a(d+1)-bd]}\right\}$$
$$+ \mathrm{Re}\left\{\frac{\mathrm{i}[2\omega_0\cos(\omega_0\tau_0) + (d-a)\sin(\omega_0\tau_0)]}{(b-a)\omega_0^2 + \mathrm{i}\,\omega_0[a(d+1)-bd]}\right\}$$
$$+ \mathrm{Re}\left\{\frac{(a-b)}{(b-a)\omega_0^2 + \mathrm{i}\,\omega_0[a(d+1)-bd]}\right\}.$$

Defining $\Gamma = \omega_0^2\{(a-b)^2\omega_0^2 + [a(d+1)-bd]^2\}$, we obtain

$$\begin{aligned}
\mathrm{Re}\left\{\left[\frac{\mathrm{d}\lambda(\tau_0)}{\mathrm{d}\tau}\right]^{-1}\right\} &= \frac{1}{\Gamma}\{(b-a)\omega_0^2[(d-a)\cos(\omega_0\tau_0) - 2\omega_0\sin(\omega_0\tau_0)] \\
&\quad + \omega_0[a(d+1)-bd][2\omega_0\cos(\omega_0\tau_0) + (d-a)\sin(\omega_0\tau_0)]\} \\
&\quad - (a-b)^2\omega_0^2 \\
&= \frac{1}{\Gamma}(d-a)\omega_0\{-(a-b)\omega_0\cos(\omega_0\tau_0) + [a(d+1)-bd]\sin(\omega_0\tau_0)\} \\
&\quad + \frac{1}{\Gamma}2\omega_0^2\{(a-b)\omega_0\sin(\omega_0\tau_0) + [a(d+1)-bd]\cos(\omega_0\tau_0)\} \\
&\quad - \frac{1}{\Gamma}(a-b)^2\omega_0^2 \\
&= \frac{1}{\Gamma}\left[(d-a)^2\omega_0^2 + 2\omega_0^4 + 2\omega_0^2 a(d+1) - (a-b)^2\omega_0^2\right].
\end{aligned}$$

Therefore,

$$\begin{aligned}
\mathrm{Re}\left\{\left[\frac{\mathrm{d}\lambda(\tau_0)}{\mathrm{d}\tau}\right]^{-1}\right\} &= \frac{\omega_0^2}{\Gamma}\left[2\omega_0^2 + d^2 - b^2 + 2a(b+1)\right] \\
&= \frac{\omega_0^2}{\Gamma}\sqrt{[2a(b+1) + d^2 - b^2]^2 - 4bd[2a(d+1) - bd]} > 0.
\end{aligned}$$

Now, we prove that for $\tau < \tau_0$, all roots of (5) have strictly negative real parts. Consider the following lemma:

Lemma A.1. *[45] The equilibrium point of the system (3) is asymptotically stable if the real parts of all eigenvalues of the characteristic equation* $Q(\lambda, \tau) = 0$ *are rigorously negative when* $\tau = 0$*, and for arbitrary real number* ω *and* $\tau' \in [0, \tau]$*,* $Q(\mathrm{i}\,\omega, \tau') \neq 0$ *holds.*

Using the above lemma, we show that the system is locally asymptotically stable. When $\tau = 0$, we can write $Q(\lambda, 0) := \lambda^2 + (d-b)\lambda - bd = 0$. Since $d > 0$ and $b < 0$, there are no roots on the imaginary axis when $\tau < \tau_0$. Therefore, according to lemma A.1, when $\tau < \tau_0$, all roots of (5) have strictly negative real parts.

Now, we demonstrate that when $\tau = \tau_0$, except for the pair of purely imaginary roots $\lambda = \pm\mathrm{i}\,\omega_0$, all roots of (5) have strictly negative parts. We prove this by contradiction. If this is not true, then there exists a pair of roots of (5) $\lambda_{1,2} = \alpha \pm \mathrm{i}\,\omega_0$, where $\alpha > 0$. Since the roots are continuous on the parameter τ, for any sufficiently small positive number ε, there exists a positive number δ such that $|\mathrm{Re}(\lambda_1) - \alpha| < \varepsilon$, when $\tau \in (\tau_0 - \delta, \tau_0 + \delta)$. Let $\varepsilon = \frac{\alpha}{2}$, we have $\mathrm{Re}(\lambda_1) > \frac{\alpha}{2}$ when $\tau \in (\tau_0 - \delta, \tau_0)$. This contradicts the stability of equilibrium for$\tau < \tau_0$.

Appendix B. Normal forms' calculations

For convenience, let $\tau = \tau_0 + \mu$ where $\mu \in \Re$, and $y_t(\theta) = y(t+\theta)$ for $\theta \in [-\tau, 0]$. Then, $\mu = 0$ is the Hopf bifurcation value for the system (3). The system can be written as a functional differential equation in $C : C([-\tau, 0], \Re^2)$ as

$$\dot{y}(t) = L_\mu y_t + F(y_t, \mu), \tag{B.1}$$

where L_μ is a linear continuous operator from C to $\Re^2$. For $\phi \in C$,

$$L_\mu \phi = B_1\phi(0) + B_2\phi(-\tau), \tag{B.2}$$

where

$$B_1 = \begin{pmatrix} a & 1 \\ a & -d \end{pmatrix}, \qquad B_2 = \begin{pmatrix} b-a & 0 \\ -a & 0 \end{pmatrix}$$

and $b = f'(x^*) < 0$. In addition, $F : C \times \Re \to \Re^2$ is

$$F(\phi, \mu) = \begin{pmatrix} b_2\phi^2(-\tau) + b_3\phi^3(-\tau) + \cdots \\ 0 \end{pmatrix}, \tag{B.3}$$

where $b_2 = \frac{1}{2}f''(x^*)$, $b_3 = \frac{1}{6}f'''(x^*), \ldots$.

By the Reisz representation theorem, for $\phi \in C$, there exists a 2×2 matrix-valued function $\eta(\theta, \mu)$ of bounded variation for $\theta \in [-\tau, 0]$, such that

$$L_\mu \phi = \int_{-\tau}^{0} \mathrm{d}\eta(\theta, \mu)\phi(\theta)\,\mathrm{d}\theta, \tag{B.4}$$

where

$$\eta(\theta, \mu) = \begin{cases} L_\mu(\phi(-\tau), \mu) & \theta = -\tau \\ 0 & -\tau < \theta \leqslant 0, \end{cases} \tag{B.5}$$

which can be satisfied by

$$\mathrm{d}\eta(\theta, \mu) = [B_1\delta(\theta) + B_2\delta(\theta+\tau)]\,\mathrm{d}\theta, \tag{B.6}$$

where $\delta(\cdot)$ is the Dirac delta function. For $\phi \in C$, we define

$$A(\mu)\phi = \begin{cases} \dfrac{\mathrm{d}\phi}{\mathrm{d}\theta} & \theta \in [-\tau, 0) \\ \displaystyle\int_{-\tau}^{0} \mathrm{d}\eta(\theta, \mu)\phi(\theta)\,\mathrm{d}\theta = L_\mu\phi & \theta = 0 \end{cases} \tag{B.7}$$

and

$$R(\mu)\phi = \begin{cases} 0 & \theta \in [-\tau, 0) \\ F(\phi, \mu) & \theta = 0 \end{cases}. \tag{B.8}$$

Since $\frac{\mathrm{d}y_t}{\mathrm{d}\theta} = \frac{\mathrm{d}y_t}{\mathrm{d}t}$, we can write (B.1) as the following ordinary differential equation as desired:

$$\dot{y}_t = A(\mu)y_t + R(\mu)y_t. \tag{B.9}$$

For $\psi \in C^1 := C([0, \tau], \Re^2)$, we define

$$L_\mu^*\psi = \int_{-\tau}^{0} \mathrm{d}\eta^T(-s, \mu)\psi(-s)d(-s). \tag{B.10}$$

The adjoint operator A^* of A is expressed as

$$A^*(\mu)\psi = \begin{cases} -\dfrac{\mathrm{d}\psi}{\mathrm{d}s} & s \in (0, \tau] \\ \displaystyle\int_{-\tau}^{0} \mathrm{d}\eta^T(-s, \mu)\psi(-s)d(-s) = L_\mu^*\psi & s = 0 \end{cases}. \tag{B.11}$$

We define the following bilinear inner product in $C \times C^1$ for $\phi \in C$ and $\psi \in C^1$:

$$\langle \psi, \phi \rangle = \langle \bar{\psi}^T(0), \phi(0) \rangle - \int_{\theta=-\tau}^{0} \int_{\xi=0}^{\theta} \bar{\psi}^T(\xi - \theta)\, \mathrm{d}\eta(\theta, \mu)\phi(\xi)\, \mathrm{d}\xi. \tag{B.12}$$

We know that $\lambda = \pm \mathrm{i}\omega_0$ are the eigenvalues of A and A^*. Let $q(\theta)$ and $q^*(\theta)$ be the eigenvectors of A and A^* associated with eigenvalues $\mathrm{i}\omega_0$ and $-\mathrm{i}\omega_0$, respectively. These eigenvectors satisfy

$$\begin{aligned} &A(0)q(\theta) = \mathrm{i}\,\omega_0 q(\theta) \\ &A(0)q^*(\theta) = -\mathrm{i}\,\omega_0 q^*(\theta). \end{aligned} \tag{B.13}$$

Let $q(\theta) = q(0)\,\mathrm{e}^{\mathrm{i}\,\omega_0\theta} = (1, \rho_1)^T\,\mathrm{e}^{\mathrm{i}\,\omega_0\theta}$ where ρ_1 is a complex value. For $\theta = 0$ and from (B.7) and (B.13), we have

$$\begin{cases} \dfrac{\mathrm{d}q(\theta)}{\mathrm{d}\theta} = \mathrm{i}\,\omega_0 q(\theta) & \theta \in [-\tau, 0) \\ L_\mu(0)q(0) = \mathrm{i}\,\omega_0 q(0) & \theta = 0 \end{cases}. \tag{B.14}$$

Therefore, from (B.2) and (B.14), we obtain

$$(B_1 - \mathrm{i}\,\omega_0 I + B_2\,\mathrm{e}^{-\mathrm{i}\,\omega_0\tau})q(0) = 0. \tag{B.15}$$

Thus,

$$\rho_1 = \frac{a(b - \mathrm{i}\,\omega_0)}{(b - a)d - a + \mathrm{i}(b - a)\omega_0}. \tag{B.16}$$

Similarly, let $q^*(\theta) = q^*(0)\,\mathrm{e}^{\mathrm{i}\,\omega_0 s} = D(\rho_2, 1)^T\,\mathrm{e}^{\mathrm{i}\,\omega_0 s}$, where ρ_2 and D are complex values. From (B.10) and (B.13), we have

$$\begin{cases} -\dfrac{\mathrm{d}q^*(s)}{\mathrm{d}s} = -\mathrm{i}\,\omega_0 q^*(\theta) & s \in [0, \tau) \\ -L_\mu^*(0)q^*(0) = -\mathrm{i}\,\omega_0 q^*(0) & s = 0 \end{cases}. \tag{B.17}$$

From (B.10) and (B.17), we can obtain

$$\left(B_1^T + \mathrm{i}\,\omega_0 I + B_2^T\,\mathrm{e}^{-\mathrm{i}\,\omega_0\tau}\right)q^*(0) = 0. \tag{B.18}$$

Therefore, we can choose

$$\rho_2 = (d - \mathrm{i}\,\omega_0). \tag{B.19}$$

We can calculate $\langle q^*, q \rangle$ as follows:

$$\begin{aligned} \langle q^*, q \rangle &= \bar{q}^{*T}(0)q(0) - \int_{\theta=-\tau}^{0} \int_{\xi=0}^{\theta} \bar{q}^{*T}(\xi - \theta)\, \mathrm{d}\eta(\theta)q(\xi)\, \mathrm{d}\xi \\ &= \bar{D}(\rho_1 + \bar{\rho}_2) - \int_{\theta=-\tau}^{0} \int_{\xi=0}^{\theta} \bar{q}^{*T}(0)\,\mathrm{e}^{-\mathrm{i}\,\omega_0(\xi-\theta)}\, \mathrm{d}\eta(\theta)q(0)\,\mathrm{e}^{\mathrm{i}\,\omega_0\xi}\, \mathrm{d}\xi\, \mathrm{d}\theta \\ &= \bar{D}(\rho_1 + \bar{\rho}_2) - \int_{\theta=-\tau}^{0} \bar{q}^{*T}(0)\, \mathrm{d}\eta(\theta)\theta q(0)\,\mathrm{e}^{\mathrm{i}\,\omega_0\theta}\, \mathrm{d}\theta \\ &= \bar{D}(\rho_1 + \bar{\rho}_2) - \bar{D}\tau\,\mathrm{e}^{-\mathrm{i}\,\omega_0\tau} \begin{bmatrix} \bar{\rho}_2 & 1 \end{bmatrix} B_2 \begin{bmatrix} 1 \\ \rho_1 \end{bmatrix} \\ &= \bar{D}\{(\rho_1 + \bar{\rho}_2) - \tau[(b - a)\bar{\rho}_2 - a]\}. \end{aligned}$$

Using $\bar{D} = 1/\{(\rho_1 + \bar{\rho}_2) - \tau[(b - a)\bar{\rho}_2 - a]\}$, we have

$$\langle q^*, q \rangle = 1. \tag{B.20}$$

In addition, since $\langle\psi, A\phi\rangle = \langle A^*\psi, \phi\rangle$, we obtain

$$-\mathrm{i}\,\omega_0\langle q^*, \bar{q}\rangle = \langle q^*, A\bar{q}\rangle = \langle A^* q^*, \bar{q}\rangle = \langle -\mathrm{i}\,\omega_0 q*, \bar{q}\rangle = \mathrm{i}\,\omega_0\langle q^*, \bar{q}\rangle.$$

Therefore,

$$\langle q^*, \bar{q}\rangle = 0. \tag{B.21}$$

Now, we apply the idea of Hassard *et al* [31] to compute the coordinates to describe the center manifold at the critical point. For y_t, a solution of (B.9) at $\mu = 0$, we define

$$z = \langle q*, y_t\rangle \qquad W(t,\theta) = y_t - zq - \bar{z}\bar{q} = y_t - 2\,\mathrm{Re}\{z(t)q(\theta)\}, \tag{B.22}$$

where z and $\bar{z}$ are the local coordinates for the center manifold in the direction of q^* and $\bar{\bar{q}}$. Note that W is real if y_t is real. We consider only real solutions. From (B.12), we obtain

$$\begin{aligned}\langle q^*, W\rangle &= \langle q^*, y_t - zq - \bar{z}\bar{q}\rangle \\ &= \langle q^*, y_t\rangle - z(t)\langle q^*, q\rangle - \bar{z}(t)\langle q^*, \bar{q}\rangle = 0.\end{aligned} \tag{B.23}$$

Therefore, for the solution of (B.9), from (B.7), (B.8) and (B.12), since $\mu = 0$, we can write

$$\begin{pmatrix}\dot{z}\\ \dot{W}\end{pmatrix} = \begin{pmatrix}\mathrm{i}\,\omega_0 & 0\\ 0 & A\end{pmatrix}\begin{pmatrix}z\\ W\end{pmatrix} + \cdot\begin{pmatrix}g(z,\bar{z})\\ H(z,\vec{z})\end{pmatrix}, \tag{B.24}$$

where

$$\begin{aligned}&f_0(z,\bar{z}) := F(W + zq + \bar{z}\bar{q}) \qquad g(z,\bar{z}) := \bar{q}^{*T}(0)f_0(z,\bar{z})\\ &H(z,\bar{z}) := \begin{cases}-q^{*T}(0)f_0(z,\bar{z}) - q^{*T}(0)\overline{f_0(z,\bar{z})} & \text{if} \quad \theta\in[-\tau,0)\\ f_0(z,\bar{z}) - \bar{q}^{*T}(0)f_0(z,\bar{z}) - q^{*T}(0)\overline{f_0(z,\bar{z})} & \text{if} \quad \theta = 0\end{cases}.\end{aligned} \tag{B.25}$$

By the Taylor expansion of the analytic function F in (B.1), we have

$$\begin{aligned}g(z,\bar{z}) &= g_{20}\frac{z^2}{2} + g_{11}z\bar{z} + g_{02}\frac{\bar{z}^2}{2} + g_{21}\frac{z^2\bar{z}}{2} + \cdots\\ H(z,\bar{z}) &= H_{20}\frac{z^2}{2} + H_{11}z\bar{z} + H_{02}\frac{\bar{z}^2}{2} + \cdots\\ W(z,\bar{z},\theta) &= W_{20}(\theta)\frac{z^2}{2} + W_{11}(\theta)z\bar{z} + W_{02}(\theta)\frac{\bar{z}^2}{2} + \cdots.\end{aligned} \tag{B.26}$$

We need to compute the values of g_{20}, g_{11}, g_{02} and g_{21}. From (B.25), we have

$$g(z,\bar{z}) = \bar{q}^{*T}(0)f_0(z,\bar{z}) = \bar{D}(\bar{\rho}_2, 1)^T\begin{pmatrix}b_2\phi_1(-\tau)^2 + b_3\phi_1(-\tau)^3\\ 0\end{pmatrix}, \tag{B.27}$$

where

$$\begin{aligned}\phi_1(-\tau)^2 &= z^2\,\mathrm{e}^{-\mathrm{i}2\omega_0\tau} + 2z\bar{z} + \bar{z}^2\,\mathrm{e}^{\mathrm{i}2\omega_0\tau} + z^2\bar{z}\big(W_{20}^{(1)}\,\mathrm{e}^{\mathrm{i}\,\omega_0\tau} + 2W_{11}^{(1)}\,\mathrm{e}^{-\mathrm{i}\,\omega_0\tau}\big) + \cdots\\ \phi_1(-\tau)^3 &= 3z^2\bar{z}\,\mathrm{e}^{-\mathrm{i}\,\omega_0\tau} + \cdots.\end{aligned} \tag{B.28}$$

Thus, we obtain

$$\begin{aligned}g_{20} &= 2\bar{D}\bar{\rho}_2 b_2\,\mathrm{e}^{-\mathrm{i}2\omega_0\tau}\\ g_{11} &= 2\bar{D}\bar{\rho}_2 b_2\\ g_{02} &= 2\bar{D}\bar{\rho}_2 b_2\,\mathrm{e}^{\mathrm{i}2\omega_0\tau}\\ g_{21} &= 2\bar{D}\bar{\rho}_2\big(b_2 W_{20}^{(1)}(-\tau)\,\mathrm{e}^{\mathrm{i}\,\omega_0\tau} + 2b_2W_{11}^{(1)}(-\tau)\,\mathrm{e}^{-\mathrm{i}\,\omega_0\tau} + 3b_3\,\mathrm{e}^{-\mathrm{i}\,\omega_0\tau}\big).\end{aligned} \tag{B.29}$$

In order to determine g_{21}, we still need to compute $W_{20}(-\tau)$ and $W_{11}(-\tau)$. Now, for $\theta \in [-\tau, 0)$,

$$\begin{aligned} H(z, \bar{z}, \theta) &= -2\,\mathrm{Re}\{\bar{q}^{*T}(0) f_0(z, \bar{z}) q(\theta)\} \\ &= -2\,\mathrm{Re}\{g(z, \bar{z}) q(\theta)\} \\ &= -g(z, \bar{z}) q(\theta) - \bar{g}(z, \bar{z}) \bar{q}(\theta) \\ &= -\left(g_{20}\frac{z^2}{2} + g_{11} z\bar{z} + g_{02}\frac{\bar{z}^2}{2} + g_{21}\frac{z^2\bar{z}}{2} + \cdots\right) q(\theta) \\ &\quad - \left(\bar{g}_{20}\frac{z^2}{2} + \bar{g}_{11} z\bar{z} + \bar{g}_{02}\frac{\bar{z}^2}{2} + \bar{g}_{21}\frac{z^2\bar{z}}{2} + \cdots\right) \bar{q}(\theta). \end{aligned}$$

When compared with $H(z, \bar{z}, \theta)$ in (B.26), we obtain

$$\begin{aligned} H_{20}(\theta) &= -g_{20} q(\theta) - \bar{g}_{02}\bar{q}(\theta) \\ H_{11}(\theta) &= -g_{11} q(\theta) - \bar{g}_{11}\bar{q}(\theta). \end{aligned} \tag{B.30}$$

By calculating the derivative of W in (B.26), we find

$$\begin{aligned} \dot{W}(\theta) &= W_z \dot{z} + W_{\bar{z}}\dot{\bar{z}} \\ &= \mathrm{i}2\omega_0 W_{20}(\theta) z^2 + \mathrm{i}\,\omega_0 W_{11}(\theta) z\bar{z} - \mathrm{i}2\omega_0 W_{02}(\theta)\bar{z}^2 - \mathrm{i}\,\omega_0 W_{11}(\theta) z\bar{z} + \cdots. \end{aligned} \tag{B.31}$$

By comparing the coefficients of z^2, $z\bar{z}$ and $\bar{z}^2$ of (B.31) with those of (B.24), we find

$$\begin{aligned} (A - \mathrm{i}2\omega_0 I) W_{20}(\theta) &= -H_{20}(\theta) \\ A W_{11}(\theta) &= -H_{11}(\theta) \\ (A + \mathrm{i}2\omega_0 I) W_{02}(\theta) &= -H_{02}(\theta). \end{aligned} \tag{B.32}$$

It follows from (B.7) and (B.32) that for $\theta \in [-\tau, 0)$,

$$\begin{aligned} \begin{pmatrix} \dot{W}_{20}(\theta) \\ \dot{W}_{11}(\theta) \end{pmatrix} &= \begin{pmatrix} A W_{20}(\theta) \\ A W_{11}(\theta) \end{pmatrix} = \begin{pmatrix} \mathrm{i}2\omega_0 I W_{20}(\theta) - H_{20}(\theta) \\ -H_{11}(\theta) \end{pmatrix} \\ &= \begin{pmatrix} \mathrm{i}2\omega_0 I W_{20}(\theta) + g_{20} q(\theta) + \bar{g}_{20}\bar{q}(\theta) \\ g_{11} q(\theta) + \bar{g}_{11}\bar{q}(\theta) \end{pmatrix} \\ &= \begin{pmatrix} \mathrm{i}2\omega_0 I W_{20}(\theta) + g_{20} q(0)\,\mathrm{e}^{\mathrm{i}\,\omega_0\theta} + \bar{g}_{20}\bar{q}(0)\,\mathrm{e}^{-\mathrm{i}\,\omega_0\theta} \\ g_{20} q(0)\,\mathrm{e}^{\mathrm{i}\,\omega_0\theta} + \bar{g}_{20}\bar{q}(0)\,\mathrm{e}^{-\mathrm{i}\,\omega_0\theta} \end{pmatrix}. \end{aligned} \tag{B.33}$$

Solving (B.33), we obtain

$$\begin{pmatrix} W_{20}(\theta) \\ W_{11}(\theta) \end{pmatrix} = \begin{pmatrix} \dfrac{\mathrm{i}g_{20}}{\omega_0} q(0)\,\mathrm{e}^{\mathrm{i}\,\omega_0\theta} + \dfrac{\mathrm{i}\bar{g}_{20}}{3\omega_0}\bar{q}(0)\,\mathrm{e}^{-\mathrm{i}\,\omega_0\theta} + E_1\,\mathrm{e}^{\mathrm{i}2\omega_0\theta} \\ -\dfrac{\mathrm{i}g_{11}}{\omega_0} q(0)\,\mathrm{e}^{\mathrm{i}\,\omega_0\theta} + \dfrac{\mathrm{i}\bar{g}_{11}}{\omega_0}\bar{q}(0)\,\mathrm{e}^{-\mathrm{i}\,\omega_0\theta} + E_2 \end{pmatrix}. \tag{B.34}$$

In addition, for $\theta = 0$, we have

$$\begin{aligned} H(z, \bar{z}, \theta) &= -2\,\mathrm{Re}\{\bar{q}^{*T}(0) f_0(z, \bar{z}) q(\theta)\} + f_0(z, \bar{z}) \\ &= -g(z, \bar{z}) q(\theta) - \bar{g}(z, \bar{z})\bar{q}(\theta) + f_0(z, \bar{z}) \\ &= -\left(g_{20}\frac{z^2}{2} + g_{11} z\bar{z} + g_{02}\frac{\bar{z}^2}{2} + g_{21}\frac{z^2\bar{z}}{2} + \cdots\right) q(\theta) \\ &\quad - \left(\bar{g}_{20}\frac{z^2}{2} + \bar{g}_{11} z\bar{z} + \bar{g}_{02}\frac{\bar{z}^2}{2} + \bar{g}_{21}\frac{z^2\bar{z}}{2} + \cdots\right)\bar{q}(\theta) \\ &\quad + f_0(z, \bar{z}). \end{aligned} \tag{B.35}$$

Hence,

$$\begin{aligned} H_{20}(0) &= -g_{20}q(0) - \bar{g}_{02}\bar{q}(0) + K_1 \\ H_{11}(0) &= -g_{11}q(0) - \bar{g}_{11}\bar{q}(0) + K_2, \end{aligned} \tag{B.36}$$

where

$$K_1 = \begin{pmatrix} 2b_2\,\mathrm{e}^{-\mathrm{i}2\omega_0\tau} \\ 0 \end{pmatrix}, \qquad K_2 = \begin{pmatrix} 2b_2 \\ 0 \end{pmatrix}. \tag{B.37}$$

From the definition of A in (B.7) and (B.32), we have

$$\begin{aligned} \int_{-\tau}^{0} \mathrm{d}\eta(\theta) W_{20}(\theta)\,\mathrm{d}\theta &= \mathrm{i}2\omega_0 W_{20}(0) - H_{20}(0) \\ \int_{-\tau}^{0} \mathrm{d}\eta(\theta) W_{11}(\theta)\,\mathrm{d}\theta &= -H_{11}(0). \end{aligned} \tag{B.38}$$

Substituting (B.34) and (B.36) into (B.38) and noting that

$$\begin{aligned} \left(\mathrm{i}\,\omega_0 I - \int_{-\tau}^{0} \mathrm{d}\eta(\theta)\,\mathrm{e}^{\mathrm{i}\,\omega_0\tau}\,\mathrm{d}\theta\right) q(0) &= 0 \\ \left(-\mathrm{i}\,\omega_0 I - \int_{-\tau}^{0} \mathrm{d}\eta(\theta)\,\mathrm{e}^{-\mathrm{i}\,\omega_0\tau}\,\mathrm{d}\theta\right) \bar{q}(0) &= 0, \end{aligned} \tag{B.39}$$

we obtain

$$\begin{pmatrix} \left(\mathrm{i}2\omega_0 I - \int_{-\tau}^{0} \mathrm{d}\eta(\theta)\,\mathrm{e}^{\mathrm{i}2\omega_0\tau}\,\mathrm{d}\theta\right) E_1 \\ \left(\int_{-\tau}^{0} \mathrm{d}\eta(\theta)\,\mathrm{d}\theta\right) E_2 \end{pmatrix} = \begin{pmatrix} K_1 \\ -K_2 \end{pmatrix} \tag{B.40}$$

or

$$\begin{pmatrix} \left(\mathrm{i}2\omega_0 I - (B_1 + B_2\,\mathrm{e}^{-\mathrm{i}2\omega_0\tau})\right) E_1 \\ (B_1 + B_2\,\mathrm{e}^{-\mathrm{i}2\omega_0\tau}) E_2 \end{pmatrix} = \begin{pmatrix} K_1 \\ -K_2 \end{pmatrix}. \tag{B.41}$$

Thus, the normal form parameters of (9) can be calculated.

References

[1] Dugard L and Verriest E I 1998 *Stability and Control of Time-Delay Systems* (London, UK: Springer)
[2] Hale J K and Verduyn Lunel S M 1993 *Introduction to Functional Differential Equations* (New York: Springer)
[3] Chen G, Molola J L and Wang H O 2000 Bifurcation control: theories, methods and applications *Int. J. Bifur. Chaos* **10** 511–48
[4] Yu P 2003 Bifurcation dynamics in control systems *Bifurcation Control: Theory and Applications* ed G R Chen, D J Hill and X Yu (Berlin: Springer) pp 99–126
[5] Pyragas K 1992 Continuous control of chaos by self-controlling feedback *Phys. Lett* A **170** 421–8
[6] Bleich M and Socolar J 1996 Stability of periodic orbits controlled by time-delay feedback *Phys. Lett.* A **210** 87–94
[7] Brandt M, Shih H and Chen G 1997 Linear time-delay feedback control of a pathological rhythm in a cardiac conduction model *Phys. Rev* E **56** 1334–7
[8] Song Y, Yu X, Chen G, Xu J and Tian Y 2002 Time delayed repetitive learning control for chaotic systems *Int. J. Bifur. Chaos* **12** 1057–65
[9] Vasegh N and Khaki Sedigh A 2008 Delayed feedback control of time-delayed chaotic systems: analytical approach at Hopf bifurcation *Phys. Lett* A **372** 5110–4
[10] Pyragas K, Pyragas V, Kiss I Z and Hudson J L 2004 Adaptive control of unknown unstable steady states of dynamical systems *Phys. Rev* E **70** 026215
[11] Hövel P and Schöll E 2005 Control of unstable steady states by time-delayed feedback methods *Phys. Rev* E **72** 046203

[12] Yanchuk S, Wolfrum M, Hövel P and Schöll E 2006 Control of unstable steady states by long delay feedback *Phys. Rev.* E **74** 026201
[13] Choe C U, Flunkert V, Hövel P, Benner H and Schöll E 2007 Conversion of stability in systems close to a Hopf bifurcation by time-delayed coupling *Phys. Rev* E **75** 046206
[14] Lu J, Ma Z and Li L 2009 Double delayed feedback control for the stabilization of unstable steady states in chaotic systems *Commun. Nonlinear Sci. Numer. Simulat.* **14** 3037–45
[15] Nakajima H and Ueda Y 1998 Limitation of generalized delayed feedback control *Physica* D **111** 143–50
[16] Socolar J E S, Sukow D W and Gauthier D J 1994 Stabilizing unstable periodic orbits in fast dynamical systems *Phys. Rev* E **50** 3245–8
[17] Hassouneh M A, Lee H C and Abed E H 2004 Washout filters in feedback control: benefits, limitations and extensions *Proc. American Control Conf. (Boston, MA, 30 June–2 July 2004)* pp 3950–5
[18] Pyragas K 2001 Control of chaos via an unstable delayed feedback controller *Phys. Rev. Lett.* **86** 2265–8
[19] Fiedler B, Flunkert V, Georgi M, Hövel P and Schöll E 2007 Refuting the odd-number limitation of time-delayed feedback control *Phys. Rev. Lett.* **98** 114101
[20] Just W, Fiedler B, Georgi M, Flunkert V, Hövel P and Schöll E 2007 Beyond the odd number limitation: a bifurcation analysis of time-delayed feedback control *Phys. Rev* E **76** 026210
[21] Huijberts H, Michiels M and Nijmeijer H 2009 Stabilisability via time-delayed feedback: an eigenvalue optimization approach *SIAM J. Appl. Dyn. Syst.* **8** 1–20
[22] Chen M Y, Han Z Z and Shang Y 2003 Another limitation of DFC when stabilizing unstable fixed points of continuous chaotic system *Phys. Lett* A **331** 501–3
[23] Balanov A G, Janson N B and Schöll E 2005 Delayed feedback control of chaos: bifurcation analysis *Phys. Rev* E **71** 16222
[24] Guan X P *et al* 2003 Time-delayed feedback control of time-delay chaotic systems *Int. J. Bifur. Chaos* **13** 193–205
[25] Sun J 2004 Delay-dependent stability criteria for time-delay chaotic systems via time-delay feedback control *Chaos Solitons Fractals* **21** 143–50
[26] Sun J 2004 Global synchronization criteria with channel time-delay for chaotic time-delay system *Chaos Solitons Fractals* **21** 967–75
[27] Park J H and Kwon O 2005 A novel criterion for delayed feedback control of time-delay chaotic systems *Chaos Solitons Fractals* **23** 495–501
[28] Park J H and Kwon O M 2006 Guaranteed cost control of time-delay chaotic systems *Chaos Solitons Fractals* **27** 1011–8
[29] Kang W 1998 Bifurcation and normal form of nonlinear control systems, parts I and II *SIAM J Control Optim.* **36** 193–232
[30] Yu P and Leung A Y T 2007 The simplest normal form and its application to bifurcation control *Chaos Solitons Fractals* **33** 845–63
[31] Hassard B D, Kazarinoff N D and Wan Y H 1981 *Theory and Applications of Hopf Bifurcation* (Cambridge, MA: Cambridge University Press)
[32] Kelly F, Maulloo A and Tan D 1998 Rate control in communication networks: shadow prices, proportional fairness and stability *J. Oper. Res. Soc.* **49** 237–52
[33] Ranjan P, Abed E H and La R J 2004 Nonlinear instabilities in TCP-RED *IEEE/ACM Trans. Netw.* **12** 1079–92
[34] Shakkottai S and Srikant R 2000 How good are deterministic fluid models of internet congestion control *Proc. IEEE INFOCOM (New York)*
[35] Li C, Chen G, Liao X and Yu J 2004 Hopf bifurcation in an Internet congestion control model *Chaos Solitons Fractals* **19** 853–62
[36] Raina G 2005 Local bifurcation analysis of some dual congestion control algorithms *IEEE Trans. Autom. Control* **50** 1135–46
[37] Wang Z and Chu T 2006 Delay induced Hopf bifurcation in a simplified network congestion control model *Chaos Solitons Fractals* **28** 161–72
[38] Yang Y H and Tian Y P 2005 Hopf bifurcation in REM algorithm with communication delay *Chaos Solitons Fractals* **25** 1093–105
[39] Guo S, Liao X and Li C 2008 Stability and Hopf bifurcation analysis in a novel congestion control model with communication delay *Nonlinear Anal.: Real World Appl.* **9** 1292–309
[40] Guo S, Liao X, Liu Q and Li C 2008 Necessary and sufficient conditions for Hopf bifurcation in an exponential RED algorithm with communication delay *Nonlinear Anal.: Real World Appl.* **9** 1768–93
[41] Chen Z and Yu P 2005 Hopf bifurcation control for an internet congestion model *Int. J. Bifur. Chaos* **15** 2643–51
[42] Xiao M and Cao J 2007 Delayed feedback-based bifurcation control in an Internet congestion model *J. Math. Anal. Appl.* **332** 1010–27

[43] Liu C L and Tian Y P 2008 Eliminating oscillations in the Internet by time-delayed feedback control *Chaos Solitons Fractals* **35** 878–87
[44] Athuraliya S, Lapsley D E and Low S H 1999 Random early marking for Internet congestion control *IEEE Proc. GLOBECOM* **3** 1747–52
[45] Cooke K and Grossman Z 1982 Discrete delay, distributed delay and stability switches *J. Math. Anal. Appl.* **86** 592–627
[46] Wright E M 1949 The linear difference-differential equation with constant coefficients *Proc. R. Soc. Edinburgh,* Sec. A: *Math. Phys. Sci.* A **62** 387–93
[47] Hale J K 1971 *Functional Differential Equations* (New York: Springer)
[48] Corless R M, Gonnet G H, Hare D E G, Jeffrey D J and Knuth D E 1996 On the Lambert W function *Adv. Comput. Math.* **5** 329–59